

Parametric investigation of pulsating blank holder's effect in deep drawing process of rectangular Al 1050 Cup

Saman Nezami¹ · Amir Akbari² · Sattar Ahangar³

Received: 27 October 2016 / Accepted: 17 June 2017 / Published online: 31 July 2017
© The Brazilian Society of Mechanical Sciences and Engineering 2017

Abstract The aim of this research is to investigate the effect of design parameters of pulsating blank holder force (PBHF) in deep drawing of an aluminum 1050 square cup in order to improve the drawing depth. Experimental tests and finite element simulations data are used to develop a second-order mathematical model to predict the drawing depth. Frequency and amplitude of the pulsating blank holder and velocity of the punch movement are considered as process variables. Individual and combined effects of these variables on the depth of drawing are investigated. The accuracy of the numerical model is verified by experimental work and statistical analysis. Optimum value of the process parameters is calculated with the aid of an empirical model. Results of this work show that frequency of the pulsation on PBHF is the most influential process parameter, and the interaction of the design variables is negligible.

Keywords Deep drawing · Pulsating blank holder · Process parameters · RSM

1 Introduction

Deep drawing is one of most common and essential sheet metal forming processes. It has a wide range of applications, varying from the production of complex automotive parts to the manufacturing of simple containers. In order to achieve an acceptable final part in deep drawing, several parameters, including the blank holder force (BHF), need to be carefully selected and designed [1, 2]. BHF controls the flow of blank material into the die cavity and plays a significant role in the deep drawing process. Using appropriate BHF is indispensable in the forming process, and applying higher or lower BHF causes wrinkling or tearing in the final part, respectively. In recent years, BHF has been subjected to several scientific works [3], and the application of variable BHF has been developed to regulate the flow of material into the die cavity in order to increase the drawing depth and prevent defects. In the industrial and automotive fields, major improvements in the critical properties of final parts, including stronger products with higher quality and significant reduction of spring back and wrinkling, have been reported as results of applying variable BHF during the forming process [4, 5]. In another study, investigation of alternating BHF on deep drawing of thin sheet metal showed that using controlled levels of BHF during the forming process can improve drawability of parts due to the reduction of ductile damage accumulation [6]. Furthermore, applying pulsation on constant BHF during deep drawing of a cylindrical cup suppresses the occurrence of wrinkling without increasing the chance of tearing, even when blank materials exhibit only a small operating window [7]. Also, the effect of introducing pulsation on blank holder when constant blank holder gap (BHG) has been used in the deep drawing process, anti-lock braking system (ABS), has been investigated. Results showed a major

Technical Editor: Márcio Bacci da Silva.

✉ Saman Nezami
sa.nezami@umbc.edu

¹ Mechanical Engineering Department, University of Maryland Baltimore County, 1000 Hilltop Cir, Baltimore, MD 21250, USA

² Department of Mechanical and Aerospace Engineering, Science and Research Branch, Islamic Azad University, Tehran, Iran

³ Manufacturing Engineering Department, University of Tabriz, Tabriz, Iran

improvement in the drawability of sheet blank while the surface quality of the final part promoted and the limited drawing ratio increased [8].

Applying variable BHF in the deep drawing process is more complicated than using constant BHF because, in addition to the main blank holding force, there are other parameters, such as frequency and amplitude of vibration, that effect the flowing quality of material during the forming process. Finite element simulations are powerful tools for developing sheet metal forming processes and can both eliminate failure in the trial and error method and reduce the cost of design by predicting appropriate process parameters to avoid failure during the forming procedures. However, simulating these processes and choosing appropriate value of influential parameters are still completed in a trial and error fashion. Also, existence of several parameters in sheet metal forming makes the simulation process time consuming and, therefore, inefficient when evaluating a large number of different designs. In order to efficiently improve the design of experiments, optimization methods can be implemented to explore the relationship between variables and the quality characteristics of the process.

Response surface methodology (RSM) is an effective optimization method that has been successfully applied in a variety of manufacturing processes [9–11]. In the case of sheet metal forming processes, the spring back effect in the “U” bending sheet metal forming process has been positively eliminated by using RSM to optimize the geometry of tools (specifically, the tool’s radii), thickness distribution, and material parameters [12]. In another study, RSM has been used to approximate appropriate amounts of initial and intermediate BHF in a deep drawing process with the time variant staircase BHF [13]. The results of their experimental and numerical works showed that the desired part can be produced by using the RSM-predicted process parameters without the occurrence of fracturing. Also, response surface methodology has been used with a design hierarchy to choose multiple process parameters in the sheet metal forming of a complex part to avoid failure while obtaining an acceptable thickness strain and desired geometry [14].

In the present work, we investigate the effect of PBHF parameters in deep drawing of rectangular aluminum cup through experiments and FEM simulation. According to results of previous studies, using PBHF is an effective method to improve drawability of sheet metal while eliminating failure [7, 8, 15]. Despite this fact, additional process parameters of PBHF make application and control of this method more complicated than using constant BHF. Therefore, understanding process parameters’ effects in deep drawing is important. Thus, in this study, RSM has been implemented to establish a mathematical model to analyze effects of these parameters. This model is used to

describe the relationship between drawing depth and variables of PBHF, including amplitude, frequency, and velocity of the punch stroke. Based on this model, appropriate process parameters are chosen to achieve the maximum drawing ratio without failure during the forming procedure.

2 Experimental setup

To perform deep drawing tests, a die unit is built for a square cupping process according to die design standards [16, 17]. This die is equipped with a cam-follower system, under the blank holder plate, to introduce pulsation on the BHF and control the material flow during the process [15]. Two springs with a combined stiffness coefficient equal to 16.8 N/mm according to ISO 10243-CS1-26-125 standard are used to generate the required BHF above the blank holder plate. Figure 1 shows the schematic view of the die assembly. Experimental tests are carried out by an AMSLER 50-ton hydraulic press. The press is equipped with measurement units for controlling amounts of stroke, velocity, and force. A 150 KW electromotor is used to rotate the cam shaft. To control and adjust the rotational speed of shaft and corresponding pulsation, an inventor apparatus is connected to the electromotor. For more accuracy, rotational speed of the cam shaft is also measured and adjusted by a DEUMO precision hand tachometer. The dimensions of the tools are listed in Table 1.

3 FEM simulation

Today, finite element simulations (FEM) are powerful tools for evaluating sheet metal forming processes, and some progresses have made it feasible to acquire reliable and accurate results from simulation [18]. Using FEM simulation in studies can reduce the frequency of failures in the trial and error processes and decrease the cost of design by predicting appropriate process parameters. In this study, ABAQUS, a commercial finite element program with the capability of analyzing large deformation and complex dynamic contacts is used for simulating the deep drawing process with PBHF [19].

3.1 Model description

A FEM model of the die setup, similar to the experimental equipment, is developed (Fig. 2). In this model, the tools are modeled as rigid objects and the blank is modeled as a deformable part using R3D4 elements. A fine mesh size is chosen in this FEM model (8280 elements in die set and 6889 elements in blank model) in order to increase simulation accuracy and guarantee convergence of the results.

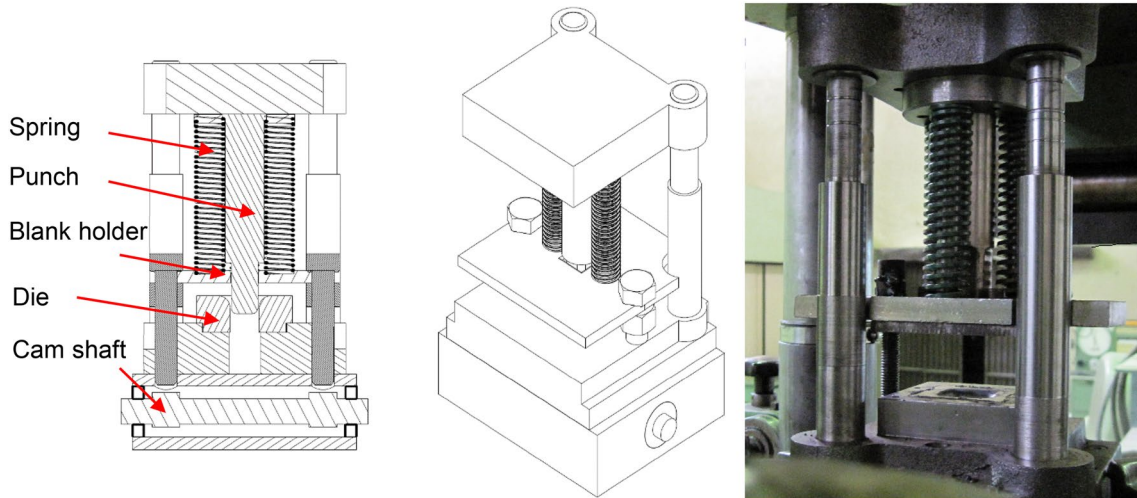


Fig. 1 Schematic view of the die assembly

Table 1 Dimensions of tools

Punch dimension (mm)	24 × 24
Die shoulder radius (mm)	5
Die dimension (mm)	25 × 25
Die shoulder radius (mm)	6

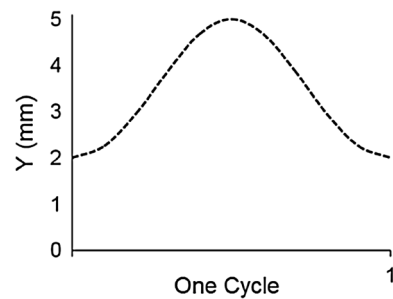


Fig. 3 Motion of cam-follower system imposed on blank holder plate

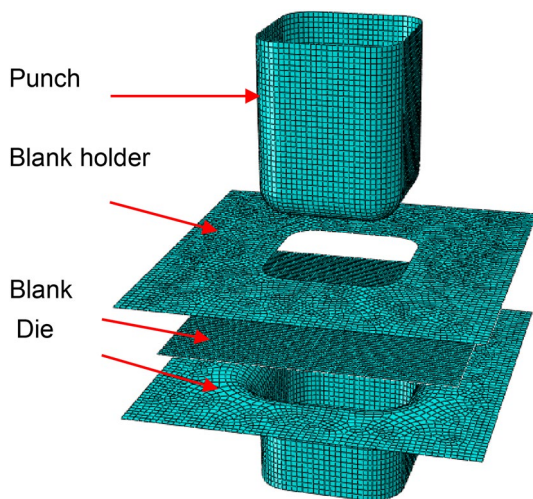


Fig. 2 FEM model of the die set

Pulsation on the blank holder is generated by periodic movement of the holder plate according to implemented cam motion in the experimental model (Eq. 1). Thus, different amplitudes and frequencies of a pulsation could be simulated through this equation for different movement conditions.

$$y = \sqrt{R^2 - e^2 \sin^2(2\pi vt)} - (r + e \cos(2\pi vt)), \quad (1)$$

where y is the amplitude; R is the radius of the cam’s outer circle; e is the distance between the center of the cam’s outer circle and the cam’s rotation center; r is the radius of the cam’s inner circle; v is the frequency and t is the time. Figure 3 shows the corresponding path that has been generated by this equation.

3.2 Model properties

During the present study, 1-mm-thick Aluminum alloy (Al 1050) is used as initial blank material. The major alloying elements are Al–0.1Fe–0.04Si–0.05Cu–0.06Zn–0.02Mn. The mechanical properties of the blank material are obtained through standard tensile testing, ASTM E8, [20] and implemented in the simulation. Table 2 shows the general mechanical properties of the blank material.

Size and shape of the initial blank are factors well-known for having a significant influence on the result of

Table 2 Material properties of the blank

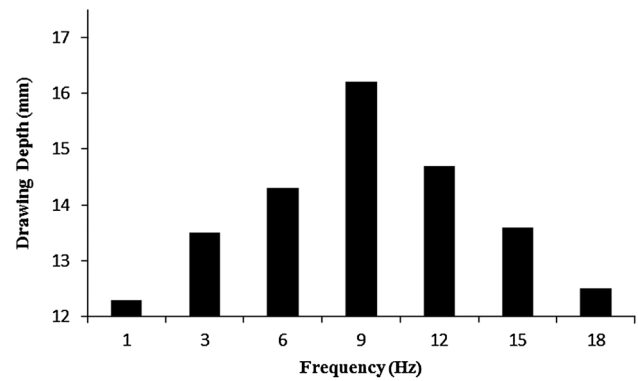
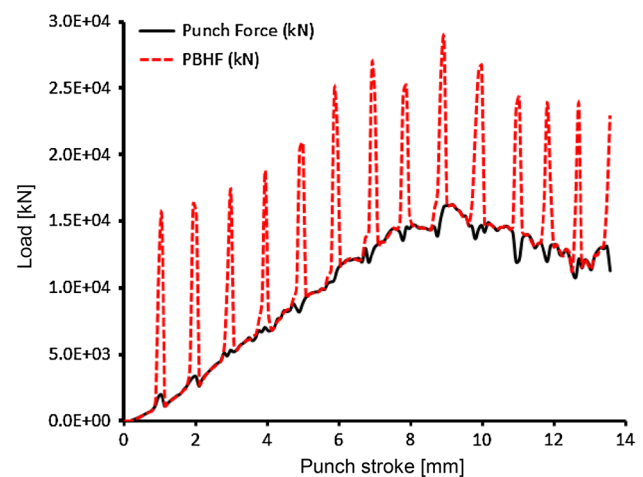
Young's modulus (GPa)	71
Yield stress, (MPa)	110
Tensile strength, (MPa)	139.4
Mass density, (kg/m ³)	2.7×10^3
Poisson's ratio	0.33

the deep drawing process [21, 22]. Determining appropriate initial blank shape and size is not the aim of this work. Thus, square blanks with dimension of 58×58 mm have been used during the simulations and experiments. The friction between the blank and the tool is simulated using an average overall simple Coulomb friction model with coefficient of friction = 0.1 [23] and surface condition of both die and punch assumed to be same while no lubrication is being used during the experiments. Wall thickness distribution is commonly used in industry for indicating the quality of a final part and it is obvious that uncontrolled wall thinning in the deep drawing process causes fracture [24, 25]. Therefore, in the present study, we used 20% wall thickness reduction as an allowable thinning limit, and exceeding this value is assumed as a failure criterion.

4 Simulation results and experimental verification

Preliminary simulation tests are carried out to find the effects of the different amplitudes and frequencies on the drawing depth. For this purpose, influence of one variable is investigated while the others are kept constant. Figure 4 shows the results of simulations for different frequencies with 3-mm constant amplitude. During all simulations, the punch speed is 0.6 mm/s. It is found that increasing frequency up to a definite level improves the drawing depth, while going beyond this level causes a negative effect on drawability. This phenomenon can be explained by the elastic retraction property of the material. When the frequency of the pulsation is at the lower level, the material is subjected mostly to plastic deformation. Then, when the frequency increases, the blank material has the opportunity to retreat elastically during each pulsation. However, when the frequency of the BHF pulsation exceeds a specific level, blank holder force applies more quickly and prevents blank material from more retraction. It is obvious that PBHF will act similarly to the constant BHF at the extra high frequencies. Figure 5 shows the effect of pulsation on BHF and punch force during a deep drawing process.

For investigating the effect of pulsation amplitude on deep drawing, different simulations with the 12 Hz pulsation frequency and 0.6 mm/s punch speed are performed.

**Fig. 4** Results of simulations for different frequencies**Fig. 5** Effect of pulsation on BHF and punch force during deep drawing process (Pulsation frequency is 12 Hz, amplitude is 3 mm and punch speed is 0.6 mm/s)

Dissimilar to the frequency, the amplitude can only be changed within a small range because of technical limitations. Figure 6 shows the effect of amplitude on the drawing depth. It can be seen that using a higher amplitude increases the drawing depth; increasing the amount of the amplitude while the maximum BHF is kept on the same level reduces the frictional force and helps material to flow easily [26].

Punch speed is one of the process parameters that also has an effect on the result of deep drawing. When the frequency of the pulsation is constant, the number of the pulsations that occur during the drawing process is inversely proportional to the punch speed. Using a higher punch speed decreases the total time of the forming process which reduces the number of pulsations during the deep drawing and vice versa. It can be seen that frequency, amplitude, and punch speed have a combined effect on the result of deep drawing, and this is discussed in Sect. 6.

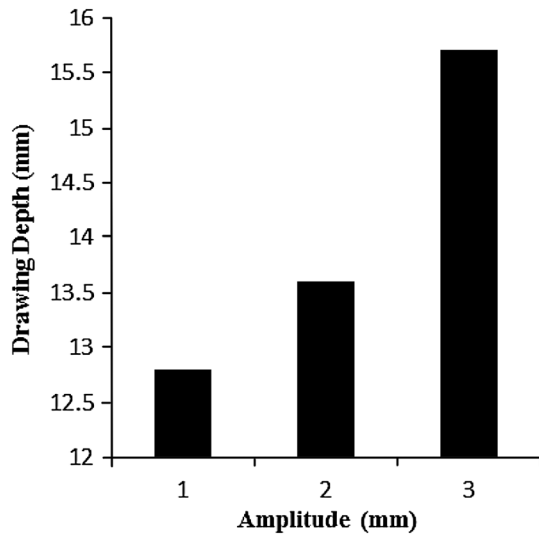


Fig. 6 Effect of amplitude on the drawing depth

It is important to verify the results of theoretical- and simulation-based studies by an experimental procedure. The results of FEM simulations are compared with the outcomes of the experimental work in order to evaluate the quality of the simulated model. Figures 7 and 8 show the corresponding results for two deep drawing processes with

Fig. 7 Results of simulation and experimental work when the frequency is 15 Hz, amplitude is 3 mm, and punch speed is 0.6 mm/s

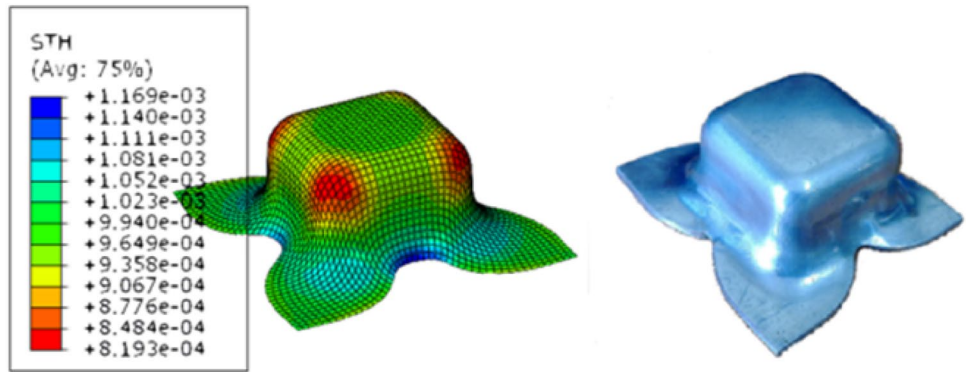
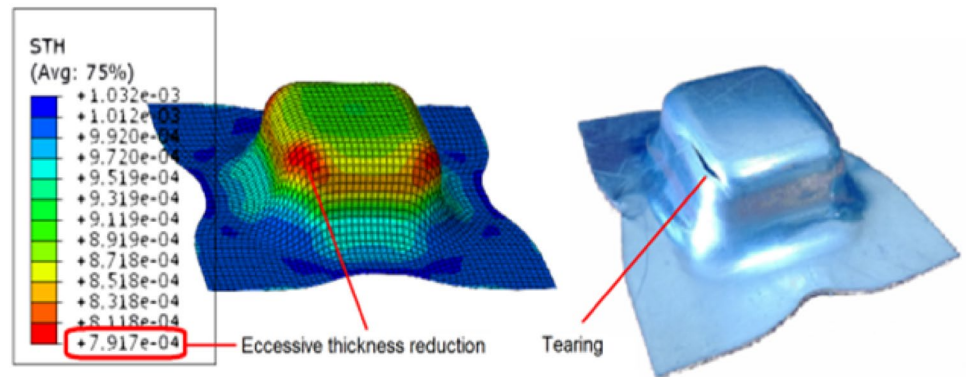


Fig. 8 Results of simulation and experimental work when the frequency is 18 Hz, amplitude is 3 mm, and punch speed is 0.6 mm/s



different frequencies. It is found that there is a good correlation between the results of the simulated and experimental works. In addition, distribution of the wall thickness of the final part for both procedures at the same forming condition has been investigated, and the results are presented in Fig. 9. As can be seen, there is good agreement between two paths; the maximum difference between simulated and experimental results is 5%, which is in the acceptable range. Figure 9 shows the effect of pulsation on BHF and punch force during the deep drawing process when frequency is 12 Hz, amplitude is 3 mm, and punch speed is 0.6 mm/s.

5 Numerical modeling

5.1 Response surface method

RSM is a modeling tool that is composed of mathematical and statistical techniques. This model is used to predict the output of a process (response variable) with respect to the several independent design parameters (input variables). In fact, one of objectives of using RSM is to optimize a process by determining appropriate value of process parameters in order to achieve any desirable output. For this aim, a series of tests (called runs) with the intended changes in

Fig. 9 Comparison of the thickness distribution in simulation and experimental work

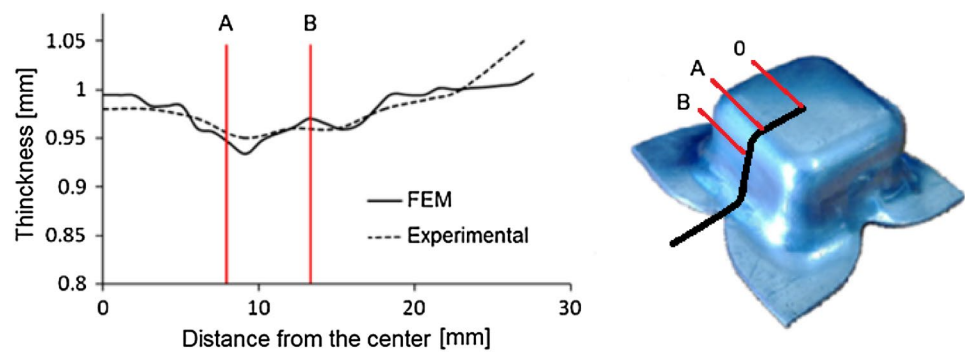


Table 3 Input variables and their levels

Variables	Unit	Coding of levels		
		-1(lowest)	0(middle)	1(highest)
Amplitude	mm	1	3	5
Velocity	mm/s	0.5	2.75	5
Frequency	Hz	1	10.5	20

the input variables should be conducted in order to identify the reasons for changes in the output response. According to the results of these tests, the relationship of the input variables and the output response can be approximated by suitable response surfaces, and the desirable output of the process can be predicted by extracting optimized input variables in advance [9, 12, 13]. Basically, the implementation procedure of RSM consists of three steps:

1. Designing a series of experiments for evaluating the response of interest.
2. Developing a response surface equation.
3. Solving the equation for the minimum or maximum response according to the selected criterion.

5.2 Design of numerical experiments

A well-designed series of experiments will reduce the total number of numerical tests and allow for simultaneous variation of independent design variables. In the current study, the Box–Behnken design, consisting of 15 experiments, is conducted to develop the mathematical model of drawing depth attained by the deep drawing process with pulsating BHF. The three design variables of pulsating BHF and their levels are given in Table 3. The results of 15 numerical tests according to the Box–Behnken are given in Table 4.

5.3 Developing response surface equation

Choosing an appropriate polynomial to fit the response equation with acceptable accuracy should be done

Table 4 Layout of numerical tests for the Box–Behnken design

Test no.	Parameters			Drawing depth <i>D</i> (mm)
	Amplitude (mm)	Velocity (mm/s)	Frequency (Hz)	
1	-1	-1	0	13.22
2	1	0	1	14.58
3	0	0	0	13.58
4	0	1	-1	8.5
5	-1	0	-1	8.37
6	-1	1	0	11.37
7	-1	0	1	10.76
8	0	1	0	13.34
9	0	0	0	13.58
10	1	-1	0	16.44
11	0	-1	-1	11.23
12	0	1	1	8.25
13	0	-1	1	10.86
14	1	0	-1	10.58
15	0	0	0	13.58

considering complexity of the problem and results of experiments. In some of the engineering problems, the response surface demonstrates some curvatures in the design variable ranges. In this study, a second-order polynomial is implemented to build the response equation, considering results of the numerical tests (Figs. 3, 4; Table 4):

$$f(x) = \beta_0 + \sum_{i=1}^k \beta_i x_i + \sum_{i=1}^k \beta_{ii} x_i^2 + \sum_{i < j} \beta_{ij} x_i x_j + \varepsilon, \quad (2)$$

where $f(x)$ is the output variable called the response variable and response design variables are represented by x_1, x_2, \dots, x_k . β is the regression coefficient; ε is the random error term, and k the number of design variables. The general form of this equation for a problem with three variables (in our study, frequency, amplitude, and velocity) is as follows:

Table 5 Coefficients of variable parameters

Term	Coefficient	Standard error	T value	P value
Constant	13.58	0.6455	21.039	0
F	0.7212	0.3953	1.825	0.128
A	1.4025	0.3953	3.548	0.016
V	-1.2862	0.3953	-3.254	0.023
F × F	-3.195	0.5818	-5.491	0.003
A × A	0.6875	0.5818	1.182	0.29
V × V	-0.675	0.5818	-1.16	0.298
F × A	0.4025	0.559	0.72	0.504
F × V	0.03	0.559	0.054	0.959
A × V	-0.3125	0.559	-0.559	0.6

Table 6 ANOVA for response equation

Source	df	Sum of square	Mean square	F ratio	P value
Regression	9	76.198	8.4466	6.76	0.024
Linear	3	33.1332	11.0444	8.84	0.019
Square	3	41.8443	13.9481	11.16	0.012
Interaction	3	1.0422	0.3474	0.28	0.84

$$f(x) = \beta_0 + \beta_1x_1 + \beta_2x_2 + \beta_3x_3 + \beta_4x_1^2 + \beta_5x_2^2 + \beta_6x_3^2 + \beta_7x_1x_2 + \beta_8x_1x_3 + \beta_9x_2x_3 + \epsilon. \tag{3}$$

The coefficients of the modeling equation are calculated in MINITAB software [27] (Table 5). Investigating second-order term coefficients in Table 5 reveals that the frequency (F^2) has the most dominant effect on response function in the deep drawing process. To evaluate the significance of the variables on the response function (drawing depth), analysis of variance (ANOVA) is performed

(Table 6). Investigating the P value of interaction in Table 6 ($0.840 > 0.05$), it can be concluded that the interactions of distinct design variables are insignificant in the response model. Thus, the interaction effect of other terms can be eliminated from the response equation. The regression equation for the response model is so obtained (Eq. 4).

$$U = 13.58 + 0.7212F + 1.4025A - 1.2862V - 3.1950F^2 + 0.6875A^2 - 0.6750V^2 + 0.4025FA + 0.0300FV - 0.3125A. \tag{4}$$

Using 95% confidence coefficient ($P < 0.05$), Eq. 4 is rewritten as follows:

$$U = 13.58 + 1.4025A - 1.2862V - 3.1950F^2. \tag{5}$$

5.4 Model adequacy control

Controlling of the fitted model is necessary to ensure the adequacy of the approximation. Examination of residuals, the difference between the observed responses and the predicted values, is a useful way for checking the capability of the model [28]. The normal probability plot (NPP), which is a graphical technique for assessing whether or not a data set is normally distributed, is used to observe normality of the residuals distribution.

Figure 10 a shows the normal probability plot of residual values. The assessment of the results' normality shows that the residual points approximately align with a straight line which confirmed the normality of the results. Also, the random distribution of the residual versus the fitted values (predicted response) in Fig. 10 b reveals that the residuals are close enough ($\text{Residuals} \leq \pm 1$) to the predicted values and verifies the adequacy of the model.

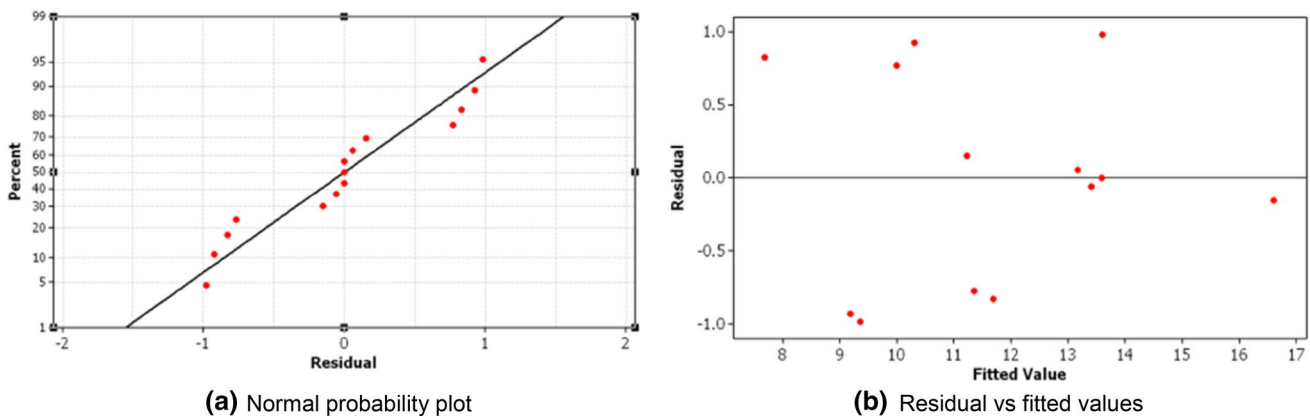


Fig. 10 Verifying accuracy of the model. **a** Normal probability plot. **b** Residual vs fitted values

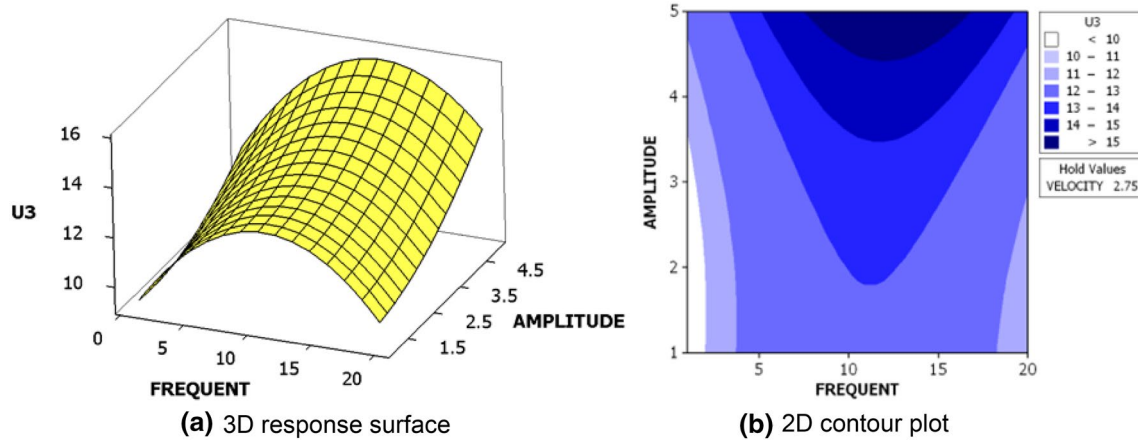


Fig. 11 Effect of pulsation amplitude (mm) and frequency (Hz) on the depth of drawing (mm). **a** 3D response surface. **b** 2D contour plot

6 Results and discussion

6.1 Analyzing response 3D surface plots and contour plots

The numerical model developed and verified in Sect. 5 provides a valuable tool to understand the effect of PBH process parameters in drawing process. In this section, 3D surface plots and 2D contour plots are built using Eq. 5 to discuss and demonstrate the influence and interaction effect of design parameters on drawing depth of the cup. Figure 11 shows the interaction effect of amplitude and frequency on the response objective. From the plots, it is clear that $U3$ (drawing depth) grows when the amplitude increases while the highest value of the $U3$ occurs at the specific region of the frequency's domain. This phenomenon can be explained by observing the polynomial model where the frequency is represented in the square form. The same tend of the $U3$ on the frequency range

is noticeable in the interactional plots of velocity and frequency (Fig. 12). It is apparent from this figure that the value of the objective response decreases when the velocity of the punch stroke increases. This is because the number of pulsations during a drawing process reduces when the bunch stroke increases. The interaction effect of amplitude and velocity of the pulsation on the drawing depth is presented in Fig. 13. These plots demonstrate that there is a positive correlation between amplitude and objective response and a negative correlation between velocity and objective response.

6.2 Optimum design values

Optimum values of the variables have been calculated by observing their relation with the objective response for achieving the highest possible value of drawing depth. Figure 14 illustrates the optimizing chart in which $U3$ varies in line with the corresponding variables and the red lines

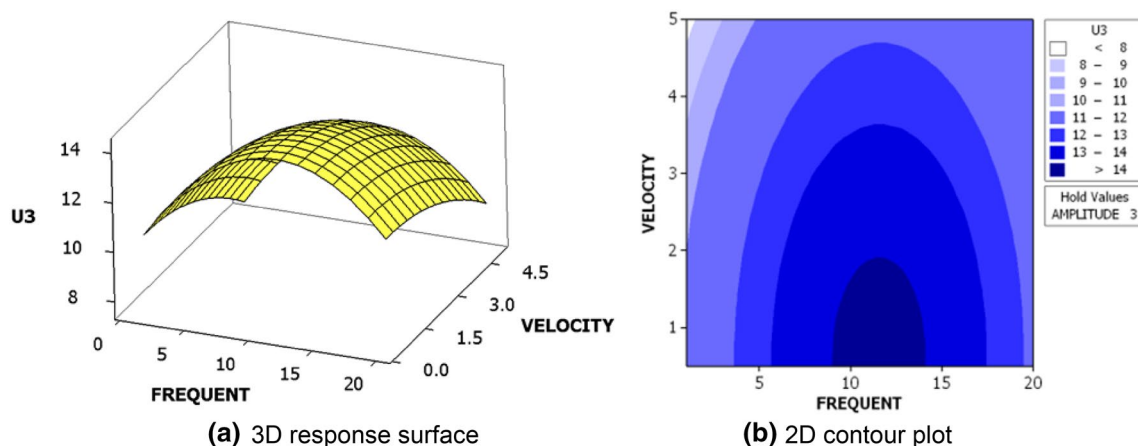


Fig. 12 Effect of pulsation velocity (mm/sec) and frequency (Hz) on the depth of drawing (mm). **a** 3D response surface. **b** 2D contour plot

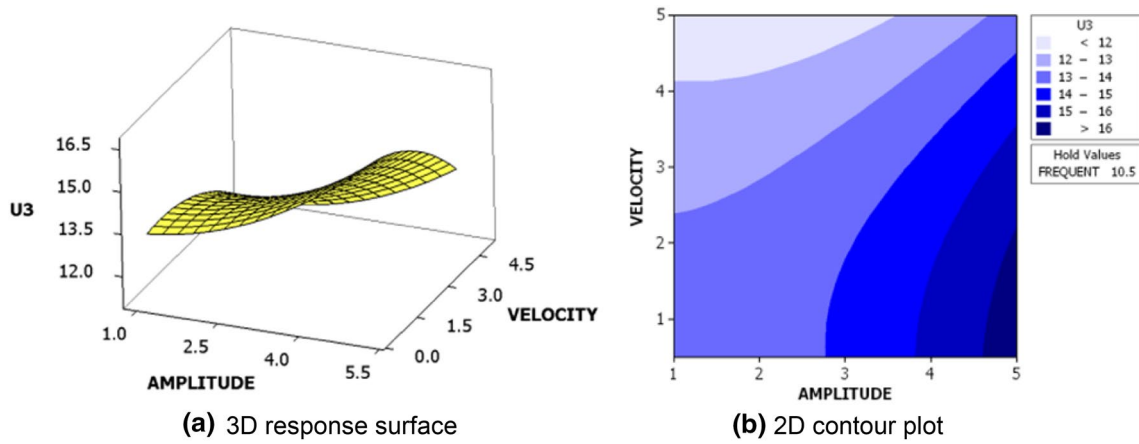


Fig. 13 Effect of pulsation amplitude (mm) and velocity (mm/s) on the depth of drawing (mm). a 3D response surface. b 2D contour plot

Fig. 14 Optimum results chart

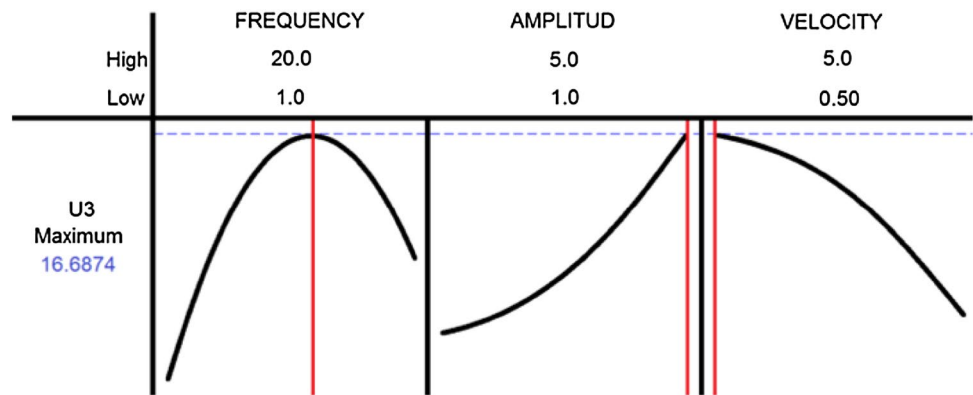


Table 7 Experimental results for verifying predicted drawing depth (mm)

Test no.	Drawing depth	Predicted	Difference	Error (%)
1	16.1	16.6874	-0.5874	3.52
2	15.8	16.6874	-0.8874	5.31
3	16.3	16.6874	-0.3874	2.32

indicate the optimum values of each variable. According to the optimization, it is found that $F = 12.1313$ Hz, $A = 5$ mm, and $V = 0.5$ mm/s are the optimum values for this engineering problem, which result in a maximum drawing depth of the cup of $U3 = 16.6874$ mm.

In order to verify the results of the proposed model, three trail experiments are conducted by using the predicted optimum values of the variables. Table 7 shows the results of these experiments compared with the predicted values. The results show that the maximum error between experimental results and predicted values is 5.31%, which is negligible.

7 Conclusion

In this study, the influence of design parameters of PBHF on drawing depth rectangular cup is investigated. Using experimental and FEM simulation data, a numerical model is built to investigate the individual and interaction effect of process parameters. It is shown that the pulsation frequency is the most dominant parameter on the depth of drawing and its optimum value needs to be calculated from the numerical model. In addition, the drawing depth increases continuously by increasing the amplitude of pulsation. In the presented die setup, three different pulsation amplitudes are used which is limited by the design of cam-follower system. In general, the maximum applicable value of amplitude can be limited by die manufacturing constraints and needs more investigation. Also it is shown that drawing depth of the cup declines by increasing the velocity of the punch stroke. The developed second-order model proved that there is no significant interaction among the frequency, amplitude of PBHF, and velocity of the punch.

Compliance with ethical standards

Conflict of interest The authors declare that they have no conflict of interest.

References

1. Padmanabhan R, Oliveira M, Alves J, Menezes L (2007) Influence of process parameters on the deep drawing of stainless steel. *Finite Elem Anal Des* 43(14):1062–1067
2. Venkateswarlu G, Davidson MJ, Tagore GRN (2010) Influence of process parameters on the cup drawing of aluminium 7075 sheet. *Int J Eng Sci Technol* 2(11):41–49
3. Obermeyer E, Majlessi S (1998) A review of recent advances in the application of blank-holder force towards improving the forming limits of sheet metal parts. *J Mater Process Technol* 75(1):222–234
4. Koyama H, Wagoner RH, Manabe K-I (2004) Blank holding force control in panel stamping process using a database and FEM-assisted intelligent press control system. *J Mater Process Technol* 152(2):190–196
5. Gunnarsson L, Schedin E (2001) Improving the properties of exterior body panels in automobiles using variable blank holder force. *J Mater Process Technol* 114(2):168–173
6. Yagami T, Manabe K, Yamauchi Y (2007) Effect of alternating blank holder motion of drawing and wrinkle elimination on deep-drawability. *J Mater Process Technol* 187:187–191
7. Ali S, Hinduja S, Atkinson J, Bolt P, Werkhoven R (2008) The effect of ultra-low frequency pulsations on tearing during deep drawing of cylindrical cups. *Int J Mach Tools Manuf* 48(5):558–564
8. Gavas M, Izciler M (2006) Deep drawing with anti-lock braking system (ABS). *Mech Mach Theory* 41(12):1467–1476
9. Yanhui Y, Dong L, Ziyang H, Zijian L (2010) Optimization of pre-form shapes by RSM and FEM to improve deformation homogeneity in aerospace forgings. *Chin J Aeronaut* 23(2):260–267
10. Hewidy M, El-Taweel T, El-Safty M (2005) Modelling the machining parameters of wire electrical discharge machining of Inconel 601 using RSM. *J Mater Process Technol* 169(2):328–336
11. Davidson MJ, Balasubramanian K, Tagore G (2008) Surface roughness prediction of flow-formed AA6061 alloy by design of experiments. *J Mater Process Technol* 202(1):41–46
12. Naceur H, Guo Y, Ben-Elchi S (2006) Response surface methodology for design of sheet forming parameters to control springback effects. *Comput Struct* 84(26):1651–1663
13. Wang L, Chan L, Lee T (2007) Process modeling of controlled forming with time variant blank holder force using RSM method. *Int J Mach Tools Manuf* 47(12):1929–1940
14. Jansson T, Nilsson L (2006) Optimizing sheet metal forming processes—using a design hierarchy and response surface methodology. *J Mater Process Technol* 178(1):218–233
15. Mostafapur A, Ahangar S, Dadkhah R (2013) Numerical and experimental investigation of pulsating blankholder effect on drawing of cylindrical part of aluminum alloy in deep drawing process. *Int J Adv Manuf Technol* 69(5–8):1113–1121
16. Lange K (1985) *Handbook of metal forming*. McGraw-Hill Book Company, New York
17. Smith DA (1990) *Die design handbook*. Society of Manufacturing Engineers, Dearborn
18. Makinouchi A, Teodosiu C, Nakagawa T (1998) Advance in FEM simulation and its related technologies in sheet metal forming. *CIRP Ann Manuf Technol* 47(2):641–649
19. ABAQUS 6.11 FEM Software (2011) [Computer software]. Dassault Systèmes Simulia Corp., Providence, RI, USA
20. ASTM E8-04 (2004) Standard test methods for tension testing of metallic materials. ASTM International, West Conshohocken, PA. <https://www.astm.org/>
21. Lee C, Huh H (1998) Three dimensional multi-step inverse analysis for the optimum blank design in sheet metal forming processes. *J Mater Process Technol* 80:76–82
22. Nezami S, Zahedi SA, Bakhshi-Jooybari M, Gorji A. Experimental and finite element investigation of blank shape effect in hydroforming. In: Proc. the 16th annual-international conference on mechanical engineering
23. Wifi A, Mosallam A (2007) Some aspects of blank-holder force schemes in deep drawing process. *J Achiev Mater Manuf Eng* 24(1):315–323
24. Sheng Z, Jirathearanat S, Altan T (2004) Adaptive FEM simulation for prediction of variable blank holder force in conical cup drawing. *Int J Mach Tools Manuf* 44(5):487–494
25. Yoshihara S, Manabe K-I, Nishimura H (2005) Effect of blank holder force control in deep-drawing process of magnesium alloy sheet. *J Mater Process Technol* 170(3):579–585
26. Siegert K, Ziegler M (1997) Pulsating blankholder forces in the deep-draw processes. *CIRP Ann Manuf Technol* 46(1):205–208
27. Minitab 17 Statistical Software (2010) [Computer software]. Minitab, Inc. <http://www.minitab.com>
28. Montgomery DC (2008) *Design and analysis of experiments*. Wiley, New Jersey